Downloaded from SAE International by Purdue University Technical Papers, Wednesday, March 12, 2025

SAE INTERNATIONAL

ARTICLE INFO
Article ID: 02-17-04-0023
© 2024 SAE International
doi:10.4271/02-17-04-0023

Fuel Efficiency Evaluation of an Off-Road Diesel Engine with an EGR Pump and High-Efficiency Turbocharger across Various Drive Cycles

Audrey Willoughby,[1] Michael Adekanbi,[1] Raghav Kakani,[1] Zar Nigar Ahmad,[1] Greg Shaver,[1] Eric Holloway,[1] Eric Haaland,[2] Matthew Evers,[2] Adam Loesch,[2] Josiah McClurg,[2] Nilesh Bagal,[3] James McCarthy,[3] and Michael Coates[3]

[1]Purdue University, Ray W. Herrick Laboratories, Department of Mechanical Engineering, USA
[2]John Deere, Waterloo, USA
[3]Eaton Corporation, Marshall and Galesburg, USA

Abstract

As regulations become more stringent, engine manufacturers are adopting innovative technologies to reduce emissions while maintaining durability and reliability. One approach involves optimizing air handling systems. Eaton developed a 48 V electric exhaust gas recirculation pump (EGRP) to reduce NO_x and CO_2 emissions while improving fuel efficiency when paired with a high-efficiency turbocharger.

This study integrates an electric EGRP and a high-efficiency turbocharger onto a 13.6L John Deere off-road diesel engine to evaluate the impact on fuel efficiency and NO_x emissions across various drive cycles including the nonroad transient cycle (NRTC), the low load application cycle (LLAC), the constant speed–load acceptance (CSLA) test, and the ramped modal cycle (RMC). The study highlights the benefits and limitations of the prototype EGRP on an off-road engine. Since the setup did not include aftertreatment systems, engine-out emissions were analyzed.

Experiments were conducted at selected operating points to achieve optimal brake thermal efficiency while keeping $BSNO_x$ within 25% of baseline values. These results helped develop a calibration map for both transient and steady-state testing.

For the CSLA tests, the time response to achieve 90% load was slower with the EGRP-equipped engine compared to the stock engine. Additionally, the NRTC, a regulatory cycle for the United States and the European Union, and the LLAC did not achieve the desired torque set points with the EGRP and high-efficiency turbocharger. The EGRP's slower-than-desired response when it decelerates led to excess EGR flow, which affected the engine's ability to produce torque. This was a key finding of the study.

The measured engine speed and engine load with the EGRP engine configuration were utilized to develop a modified version of the NRTC and LLAC, referred to in this article as the modified NRTC and the modified LLAC. The modified NRTC and modified LLAC were run on the stock engine to accurately compare the performance of the stock hardware with the EGRP and high-efficiency turbocharger hardware for the same transient cycles, albeit cycles that are no longer specifically the regulatory NRTC and LLAC cycles. The intent of the modified LLAC and the modified NRTC is to show what the possible benefits of EGRP and high-efficiency turbocharging may likely be if the transient response shortcoming of the EGRP is addressed

BSFC improved with the EGRP and high-efficiency turbocharger hardware for the modified NRTC, modified LLAC, and RMC. The modified NRTC showed a 1.3% improvement, the modified LLAC exhibited a 2.5% improvement, and the RMC demonstrated a 1.3% improvement. $BSNO_x$ increased by 12.9% for the modified NRTC, decreased by 11.1% for the modified LLAC, and increased by 2.8% for the RMC with the EGRP configuration. The BSPM increased by 34.2% for modified LLAC and improved by 33.1% for the modified NRTC.

History

Received: 16 May 2024
Revised: 08 Aug 2024
Accepted: 21 Nov 2024
e-Available: 10 Dec 2024

Keywords

Exhaust gas recirculation pump, NRTC, LLAC, CSLA, Engine electrification, Emission reduction, Off-road diesel engine

Citation

Willoughby, A., Adekanbi, M., Kakani, R., Ahamd, Z. et al., "Fuel Efficiency Evaluation of an Off-Road Diesel Engine with an EGR Pump and High-Efficiency Turbocharger across Various Drive Cycles," *SAE Int. J. Commer. Veh.* 17(4):397-415, 2024, doi:10.4271/02-17-04-0023.

ISSN: 1946-391X
e-ISSN: 1946-3928

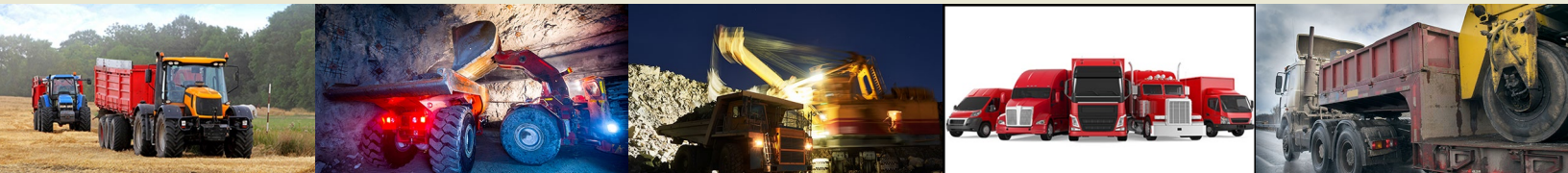

Downloaded from SAE International by Purdue University Technical Papers, Wednesday, March 12, 2025

Introduction

The reliance on diesel engines across various sectors such as agriculture, construction, mining, and forestry is driven by the diesel engine's notable attributes: high thermal efficiency, high-power output capacity, and robust durability [1]. Unfortunately, diesel engines emit harmful pollutants, including particulate matter (PM) and nitrogen oxides (NO_x) [2]. Inhaling PM can exacerbate respiratory allergic reactions, while high exposure to NO_x can damage respiratory airways [3, 4]. Beyond the health impacts of NO_x, it constitutes environmental concerns of ozone depletion [5]. In 2023, approximately 1,557,000 tons of NO_x were produced by off-road vehicles, constituting roughly 23% of the national emission total [6].

To address these environmental and health challenges, regulatory bodies like the U.S. Environmental Protection Agency (EPA) and the California Air Resources Board (CARB) have enacted increasingly stringent emission standards. Shortly after the completion of this study, CARB proposed Tier 5 Emission Standards, requiring up to 90% reductions in NO_x and 75% reductions in PM, respectively, contingent upon the power category [7].

Original engine manufacturers are complying with existing Tier 4 Emission Standards for NO_x by utilizing high-pressure-cooled exhaust gas recirculation (EGR). This method entails circulating exhaust gas through an EGR cooler before reintroducing it back into the engine [1]. EGR effectively reduces the oxygen concentration and flame temperature, thereby lowering NO_x formation [8, 9, 10]. However, driving EGR necessitates a turbocharger to maintain back pressure on the engine, resulting in increased fuel consumption [8, 9, 10].

Eaton's Electric Generation 3 EGR pump (EGRP) eliminates the need for positive engine delta pressure to facilitate EGR [11]. The less-efficient turbocharger can be replaced with a high-efficiency turbocharger to reduce the engine delta pressure, improve the pumping work, and enhance the fuel economy.

Experimental Setup

To evaluate the benefits of the new technology, the EGRP and a twin-scroll high-efficiency turbocharger were implemented on a 13.6L John Deere Engine in Herrick Laboratories at Purdue University.

The EGRP, depicted in Figure 1, is a rotary positive displacement pump adapted from Eaton's supercharger technologies [11, 12]. Equipped with a 48 V motor, the EGRP can sustain continuous power of up to 3 kW, either generating or consuming power [12]. In already deployed applications, there are existing battery and hybrid electric vehicle systems that provide voltage to electric components in commercial off-road vehicles [13, 14, 15]. The EGR flow rate can be adjusted by varying the commanded EGRP speed through a controller area network (CAN) signal [12]. The specifications on the pump are shown in Table 1. To power the pump, a regenerative power supply was utilized. Additionally, a specialized coolant cart, developed by the Eaton Team, was employed to continuously circulate coolant through the pump at approximately 60°C.

FIGURE 1 Eaton's Electric Generation 3 exhaust gas recirculation pump.

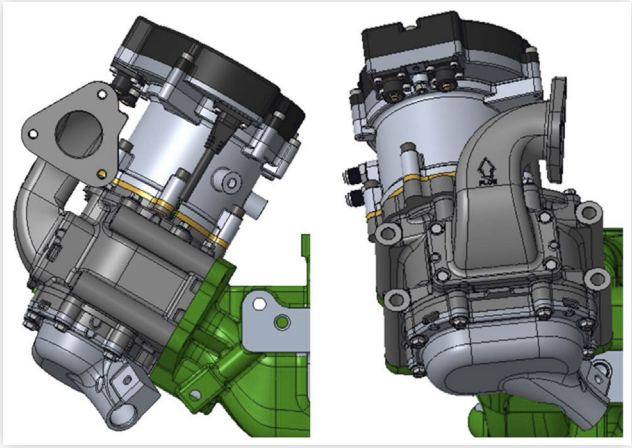

Reprinted with permission from Ref. [12]. © Eaton Corporation

The 510 kW engine utilized an EGR valve, twin turbochargers in series, and a boost control solenoid. The boost control solenoid (BCS), commonly used as an active waste gate system [16], was employed on the high-pressure turbine to control and regulate the boost pressure. Details regarding the specifications of the diesel engine can be found in Table 2.

Additional hardware was incorporated into the system, including a split exhaust manifold and an intercooler. The split exhaust manifold segregated exhaust gas from cylinders 1–3 to cylinders 4–6. Meanwhile, the intercooler, positioned between the low-pressure compressor and the high-pressure compressor, served to reduce the amount of work required to compress fresh air. Lab-grade pressure, temperature, and flow rate measurements were collected via Speedgoat. Engine control unit (ECU) data was obtained through CAN and John Deere's software, while EGRP data was collected via CAN. MATLAB and Simulink software were used for data analysis.

TABLE 1 Eaton's Electric Generation 3 exhaust gas recirculation pump specifications.

Parameter	Nominal specification
Pump revision level	Gen 3
Motor revision level	New 3 kW motor
Nominal power rating	3 kW (continuous)
Pump displacement	400 cc/rev
Power interface	48 VDC
Lubrication	Engine oil
Cooling	Engine coolant
Communication interface	CAN
Maximum operating speed	10,000 rpm
Power recovery	Available up to power rating
Assembly mass	27 kg

Reprinted with permission from Ref. [12]. © Eaton Corporation

Downloaded from SAE International by Purdue University Technical Papers, Wednesday, March 12, 2025

TABLE 2 John Deere's 13.6 diesel engine specifications.

Performance data	
Rated power	510 kW (684 hp)
Rated speed	2100 rpm
Peak torque	3050 Nm (2250 lb-ft) at 1550 rpm
General data	
Type	6-cylinder, in-line, 4-stroke, water-cooled
Bore and stroke	132 × 165 mm
Fuel system	Electronic high-pressure common rail (HPCR)
Aspiration	Turbocharged, air-to-air aftercooled
Turbo	Series (fixed, wastegate)
EGR	External cooled exhaust gas recirculation (EGR)
Emission level	EPA final Tier 4/EU Stage V

Data taken from Ref. [17]. © SAE International

Fuel consumption was calculated by measuring the weight difference using a load cell and fuel bucket. John Deere's NO_x OEM Sensor was utilized in measuring NO_x emissions, with the relative accuracy being ±10%, at a particular reading. The specifications of the instrumentation used are provided in Table 3. Figure 2 presents the test cell schematic, incorporating the EGRP and high-efficiency turbocharger, along with the locations for pressure and temperature measurements.

Drive Cycles

Different transient cycles were used to assess emissions and fuel consumption. In this study the following transient tests were employed in experimental testing: the constant speed–load acceptance (CSLA) test, the nonroad transient cycle (NRTC), the low load application cycle (LLAC), and the ramped modal cycle (RMC). The cycles were selected based on relevance and importance to the regulatory bodies [18, 19, 20].

Depending on the off-road application, a nonroad engine may experience dynamic changes in engine speed and engine load such as a crawler tractor, while other applications, like the agricultural tractor, do not encounter the drastic changes in engine speed and load, but require the ability to quickly produce power and sustain that high power, as shown in Figure 3 [21].

TABLE 3 Specification of instrumentation used in experiments at Purdue.

Instrument	Measured parameter	Measurement range
AC dynamometer	Speed	0–3000 rpm
	Torque	0–5000 Nm
Laminar flow element	Air flow rate	0–2300 kg/h
K-type thermocouple	Temperature	−200–1260°C
Pressure transducer	Pressure	0–5 bar/0–8 bar
Weighing balance	Diesel consumption	36,300 g
John Deere NO_x sensor	NO_x measurement	0–2000 ppm
AVL MSS 483	PM concentration	0–50 mg/m^3

© SAE International

The CSLA test is utilized to access the time response to 90% load and examine the peak soot measurement during the transient response. It helps determine how quickly the engine can increase output torque while the engine dynamometer maintains a constant speed. The throttle is snapped a total of three separate times to reach 100% load for a specified engine speed. Figure 4 is an example of the CSLA test for the 1900 rpm operating point.

To rapidly generate torque, fuel is injected early into the cylinder [22]. Excess fuel injected into the cylinders can lead to incomplete combustion resulting in higher peak soot measurements [22]. The main objective of the CSLA test is to minimize the time required to achieve 90% load while keeping peak soot emissions within acceptable limits.

Variations in engine speed and brake torque are typical in off-road applications, impacting both fuel consumption and emission levels in diesel engines [23]. In an effort to have a more representative cycle to measure emissions from nonroad activity, the U.S. EPA, in collaboration with the Engine Manufacturer's Association (EMA) and the Southwest Research Institute (SwRI), developed the NRTC [24]. This cycle encompasses various off-road duty cycles including a backhoe loader, a rubber tire loader, a crawler-dozer, an agricultural tractor, an excavator, an arc welder, and a skid steer loader [24, 25]. The NRTC serves as a standardized cycle for the U.S. EPA Tier 4 and EU Stage V emission standards [24, 26]. This test assesses emissions from compression ignition engines used in nonroad machinery under dynamic conditions. The NRTC consists of a cold start, a 20-min soak, and a hot start, featuring significant variations in speed and torque, making it one of the most rigorous transient cycles compared to other legislative tests [24, 27]. In the United States, emissions are calculated by adding 5% of the cold start emissions with 95% of the hot start emissions, while the EU's Stage IV certification uses 90% hot mode and 10% cold mode [24, 26, 28]. In this study, the analysis of the NRTC focuses on the hot start. The cold NRTC was outside the scope of this particular study due to the small modest impact it has on fuel consumption.

The concern regarding overall cycle emissions was addressed by ensuring that, when the engine was equipped with the EGRP and high-efficiency turbocharger, the following conditions were met compared to the stock engine: (1) the engine exhaust throttle outlet temperature and exhaust mass flow rate were maintained, ensuring adequate thermal management; (2) the $BSNO_x$ and BSPM, for both configurations in steady state, were either similar or lower for most operating points, ensuring tailpipe emissions were no worse than the baseline case. The NRTC was run twice for repeatability. The normalized speed and torque of the NRTC are shown in Figure 5.

Another cycle based on real-life applications is the LLAC. This cycle was developed after CARB requested that SwRI evaluate a

Downloaded from SAE International by Purdue University Technical Papers, Wednesday, March 12, 2025

FIGURE 2 Test cell schematic of the EGRP and high-efficiency turbocharger configuration with sensor locations.

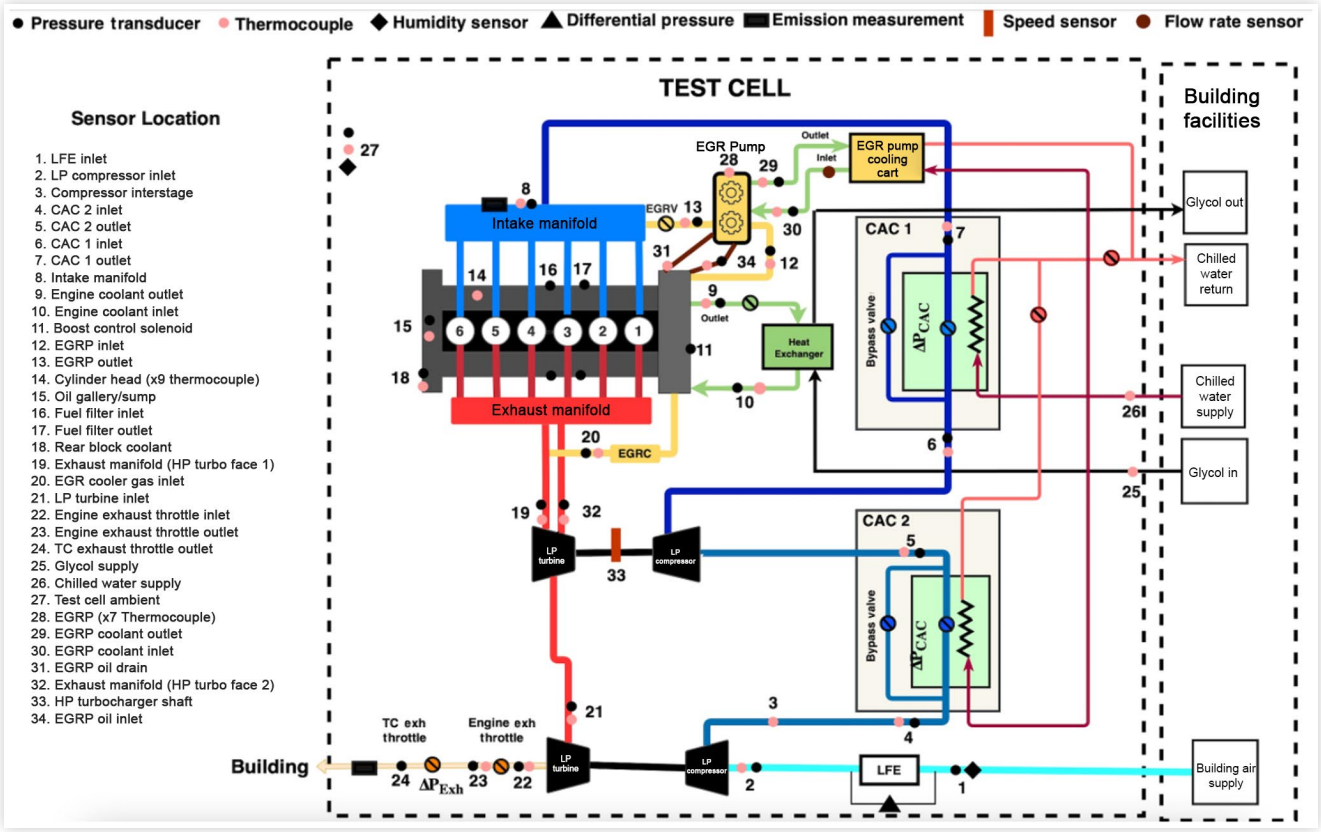

© SAE International

FIGURE 3 The normalized speed and torque for a crawler tractor cycle and agricultural tractor cycle.

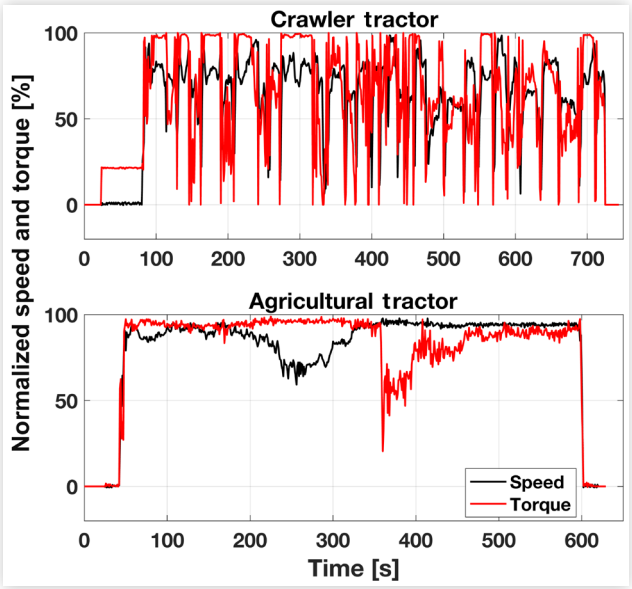

Adapted from Ref. [21]

FIGURE 4 An example of the constant speed–load acceptance test specifically for the 1900 rpm operating point.

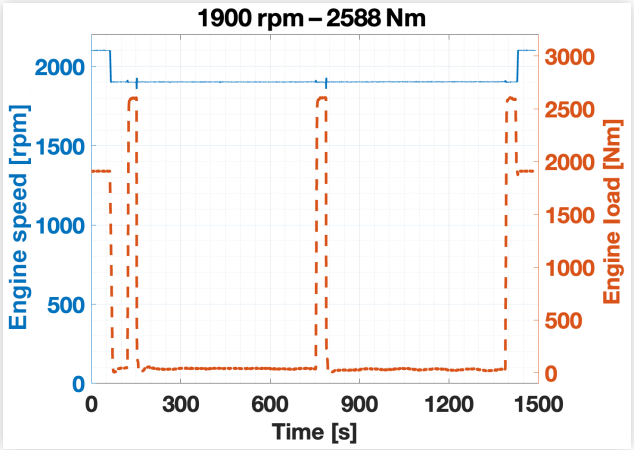

© SAE International

Downloaded from SAE International by Purdue University Technical Papers, Wednesday, March 12, 2025

FIGURE 5 Normalized speed and torque of the NRTC used in Tier 4 and Stage IV regulatory testing to analyze fuel efficiency, $BSNO_x$, and BSPM.

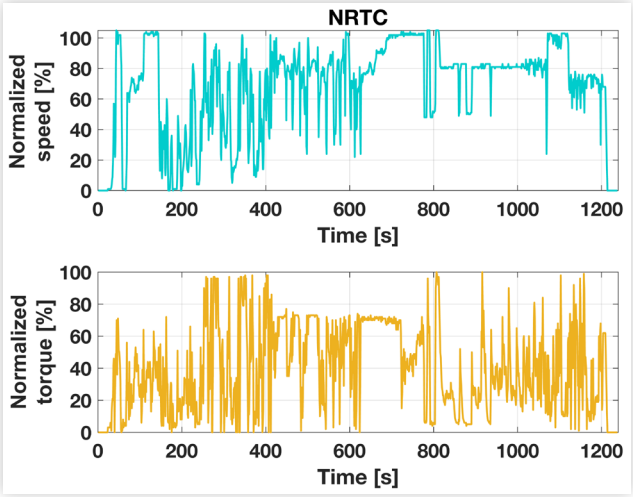

Data taken from Ref. [18]. © SAE International

FIGURE 6 Normalized speed and torque of the LLAC developed by the Southwest Research Institute to analyze fuel efficiency, $BSNO_x$, and BSPM for typical low load operations.

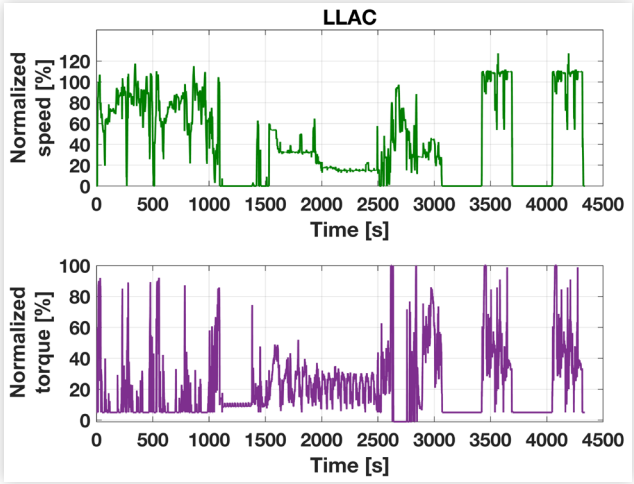

Data taken from Ref. [29]. © SAE International

typical low average load operation on engines, with aftertreatment systems, based on real-life scenarios [29]. With no cycle available at the time, SwRI, in collaboration with John Deere, designed the cycle based on 24 different application duty cycles [29]. The LLAC's average load of maximum power, at 15%, is considerably lower compared to the NRTC at 35% [29]. After the LLAC was performed on two separate engines, SwRI discovered that the emission control for NO_x at lower loads was poor, resulting in more than three to four times the regulatory emission standard [29]. With this knowledge, the LLAC was run on the 13.6L engine at Purdue with the stock engine configuration and the EGRP and high-efficiency turbocharger engine configuration. This is not only to determine if there was a fuel benefit with the EGRP, but also if the $BSNO_x$ and the exhaust throttle outlet temperature remained similar to the baseline setup. Figure 6 shows the normalized speed and torque for the LLAC.

Unlike the NRTC and LLAC, the RMC does not contain drastic transient responses. The RMC is a continuous cycle that starts at idle and smoothly ramps to each required steady-state operating point within a 20 s timeframe [24]. The steady-state points in the RMC are intentionally arranged to alternate between high and low torque to have consistent aftertreatment temperatures [24]. Table 4 lists the steady-state operating points and transitions for the RMC.

Original engine manufacturers have the option to run RMC, in contrast to steady-state discrete-mode tests, as a method of steady-state certification within the U.S. EPA Tier 4 Emission Standard [30]. The RMC was run in this study to evaluate the fuel savings with the EGRP configuration based on a continuous cycle.

Literature Review

Several studies have examined the interaction between advanced EGR systems and turbocharged diesel engines under transient conditions. For example, Gu and Su [31] performed a transient bench test on a two-stage turbocharged heavy-duty diesel engine to optimize its performance during a load increase from 20% to 100% in 1 s at a constant speed of 1200 rpm. The results indicated that using a low-pressure EGR system in the transient control scheme led to a 42.1% reduction in peak soot emission, a 24.8% decrease in peak NO_x emission, a 9.14% reduction in indicated specific fuel consumption, and a 30.6% increase in maximum IMEP achieved within 1 s,

TABLE 4 The ramped modal cycle operating points.

RMC mode number	Time in mode (s)	Engine speed (%)	Engine brake torque (%)
1a Steady-state	126	Idle	0
1b Transition	20	Linear transition	Linear transition
2a Steady-state	159	Intermediate	100
2b Transition	20	Intermediate	Linear transition
3a Steady-state	160	Intermediate	50
3b Transition	20	Intermediate	Linear transition
4a Steady-state	162	Intermediate	75
4b Transition	20	Linear transition	Linear transition
5a Steady-state	246	100%	100
5b Transition	20	100%	Linear transition
6a Steady-state	164	100%	10
6b Transition	20	100%	Linear transition
7a Steady-state	248	100%	75
7b Transition	20	100%	Linear transition
8a Steady-state	247	100%	50
8b Transition	20	Linear transition	Linear transition
9 Steady-state	128	Idle	0

Data taken from Ref. [18]. © SAE International

Downloaded from SAE International by Purdue University Technical Papers, Wednesday, March 12, 2025

compared to the steady-state optimization control scheme without EGR [31].

Liu et al. [32] studied the impacts of different intervention speeds and timings of an electric supercharger on the transient performance of a turbocharged diesel engine. To develop an optimized control strategy, simulation was used to analyze the combined impact of the electric supercharger and turbocharger. The optimized slope control strategy enhanced transient responsiveness and stability, reducing the intake pressure rise time by 52.5% compared to the base engine and significantly minimizing fluctuations in intake pressure and engine torque.

To evaluate the replacement of the EGR valve with a turbine and quantify the potential benefits of increased EGR rates and improved brake specific fuel consumption (BSFC) in a heavy-duty engine, a simulation-based assessment was conducted by Serrano et al. [33]. The results, based on eight engine running conditions, show that twin-turbocharging with compressors in series and the EGR turbine discharging after the first stage allows for approximately 5% higher maximum EGR rates and up to 7% fuel savings compared to a single-stage turbocharging layout.

Zhang et al. [34] conducted an experiment on a two-stage series turbocharged heavy-duty diesel engine with a high-pressure common rail. During the transient process, the speed was maintained at 1650 rpm, and the load was linearly increased from 10% to 100% within 5 s. The results showed that the optimized EGR valve open-loop control strategy significantly improved air–fuel mixing quality and reduced the smoke opacity peak by over 64%. With the EGR valve closed-loop control strategy, the smoke opacity peak was lower than with the open-loop control strategy but higher than without EGR.

Gumus and Otkur [35] evaluated the feasibility of using a high-efficiency compact microchannel heat exchanger as an EGR cooler to meet EURO 7 emission standards for heavy-duty diesel engines. The implementation of the newly designed microchannel heat exchanger resulted in a 6.75% reduction in NO_x emissions, an 11.30% reduction in PM emissions, and a 0.65% decrease in specific fuel consumption at the analyzed rated power operating point. These results align well with the goals for reducing NO_x and PM emissions to meet Euro 7 diesel emission regulations.

With the increase in the stringency in emission regulations, it is expedient to continue to study the performance of new technologies during transient operations, commonly experienced in actual driving conditions. Researchers have investigated and published enhancements in BSFC, brake specific nitrogen oxides ($BSNO_x$), and brake specific carbon dioxide ($BSCO_2$) using Eaton's electric EGRP in conjunction with a high-efficiency turbocharger for on-road engines [11, 36].

Johnson et al. [11] explored the advantages of integrating a high-efficiency turbocharger with an electric EGRP to optimize the air handling system. This combination improved engine fuel efficiency without increasing engine-out NO_x emissions. The study employed a variable geometry turbine (VGT) turbocharger and focused on 13 modes of the SET cycle in a steady state. The results, obtained from testing a 13L 2019 model year engine on a dynamometer, demonstrated the potential for a 3.5% reduction in engine BSFC under highway cruising conditions.

Bagal and Bhardwaj [10] examined the development and performance of the EGRP, which enhances engine fuel efficiency without increasing engine-out NO_x emissions. They utilized computational fluid dynamics to optimize Eaton's EGRP design, leading to a reduction in the pump's fluid-borne noise. This optimized design was then evaluated for fuel benefits using a calibrated GT-POWER engine model, representing a current production 13-L HD diesel engine. The newly optimized engine architecture with an Eaton EGRP demonstrated a maximum BSFC improvement of 6.2% at a 1500 rpm full load operating condition and a 4.35% fuel benefit for the 13-mode ESC engine dyno cycle.

Bistis et al. [36] demonstrated an improved CO_2 impact by utilizing high-efficiency turbochargers and an EGRP. They developed two high-efficiency turbochargers to replace the VGT turbocharger, along with an EGRP to drive the required amounts of EGR. Both turbochargers are fixed geometry without a wastegate device and were designed to reduce CO_2 emissions. The FTP and beverage transient cycles were considered in this test. However, for the FTP evaluation, the engine required a slight derate due to the engine controller limiting fuel. The first high-efficiency turbocharger achieved a 1.7% reduction in CO_2 while maintaining tailpipe NO_x slightly below 0.02 g/hp-h in the federal test procedure (FTP) cycle and a 25.7% reduction in CO_2 while NO_x decreased from 0.014 g/hp-h to 0.013 g/hp-h. The second high-efficiency turbocharger enabled a larger 3.6% reduction in CO_2 while keeping tailpipe NO_x slightly below 0.015 g/hp-h for the FTP cycle and a 27.6% reduction in CO_2 while NO_x increased from 0.014 g/hp-h to 0.020 g/hp-h for the beverage cycle.

Although there are publications on the implementation of the EGRP and high-efficiency turbocharger for on-road heavy-duty diesel engine cycles, there are no studies exploring their application to off-road diesel engine cycles such as the NRTC, LLAC, or RMC. While the FTP for heavy-duty vehicles features a greater maximum load increase (from 0% to 78.5%) compared to the NRTC (which increases from 0% to 44%), the NRTC is more dynamic [25]. The FTP heavy-duty transient cycle has 11.9 load increases per minute, while the NRTC has 23.1 [25]. Other heavy-duty drive cycles, such as the ETC (18.9 load increases per minute) and the WHTC (16.3 load increases per minute), still fall below the NRTC in terms of load increase frequency [25]. The NRTC also has the highest average normalized speed and average torque compared to other legislated heavy-duty engine cycles [25].

Hence, this work contributes to existing literature by investigating how the electric EGRP and high-efficiency turbocharger perform under various transient drive cycles that apply to off-road engines. It also seeks to demonstrate the capabilities and shortcomings of the prototype EGRP and high-efficiency turbocharger across the drive cycles on a very relevant off-road engine. For comparison purposes, the NRTC

Downloaded from SAE International by Purdue University Technical Papers, Wednesday, March 12, 2025

and LLAC cycles were modified to be less aggressive, after the EGRP and high-efficiency turbocharger were found to have transient response shortcomings. This helps to demonstrate the benefits of EGRP and turbocharging amid transient response challenges of the original NRTC and LLAC cycles. In this work, hydrocarbon emission was not measured, as they are not problematic in modern diesel engines.

Methodology

Design of Experiments

Before any testing with the EGRP and high-efficiency turbocharger could commence, the ECU control logic had to be developed. The John Deere Team effectively developed transient capable controls integrating the EGRP into existing production model-based air and EGR controls. The EGR valve position was set fully open during engine testing with the EGRP and high-efficiency turbocharger. A design of experiments (DOEs) were conducted using these controls to optimize fuel efficiency at specific operating points, while maintaining $BSNO_x$ to be within 25% of baseline values. Additional limits included maintaining engine-out temperatures similar to baseline values, staying below specific peak cylinder pressures, and other design limit requirements.

The various DOE operating points, shown in Figure 7, were tested in an open loop. The selected operating points primarily consist of points within the NRTC. The operating points were chosen for their effectiveness in developing models that define the design space and improve fuel efficiency for steady-state testing and the NRTC.

To address the concern of not incorporating an aftertreatment system into the setup, measures were taken to ensure that, when the engine was equipped with the EGRP and high-efficiency turbocharger, it performed comparably to the stock engine. Specifically, the engine exhaust throttle outlet temperature and exhaust mass flow rate were maintained at levels similar to the stock engine, ensuring that the thermal management of the aftertreatment was not inferior to the baseline case. Additionally, the engine-out $BSNO_x$ and BSPM were found to be either similar to or lower than those of the stock engine, which, in conjunction with the previous measure, indicated that the tailpipe emissions would not be expected to be worse than the baseline case.

FIGURE 7 Operating points for the design of experiments.

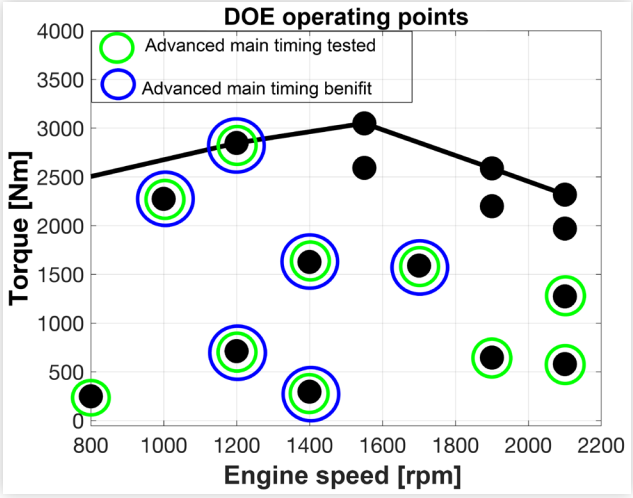

© SAE International

The DOEs entailed constraining one parameter while modifying another. For operating points below 712 Nm, the EGRP speed and the exhaust throttle area were altered to investigate the improvements in fuel economy while maintaining similar exhaust throttle outlet temperatures as the stock engine. For operating points above 712 Nm, the EGRP speed and the BCS current were primarily constrained to analyze the effects engine delta pressure and air-to-fuel ratio have on BSFC improvement and brake thermal efficiency. In certain DOEs where higher cylinder temperature and pressure were permissible, a third variable, main injection timing, was introduced. Main injection timing was advanced in efforts to enhance the combustion process and improve closed-cycle efficiency. The drawback to advancing the main timing is the increase in NO_x emissions. However, one advantage of the EGRP is the ability to reduce NO_x emissions by increasing the EGRP speed, thereby increasing the EGR flow rate. The green circles in Figure 7 represent where advanced main timing was tested. The blue circles represent operating points where advanced main timing improved fuel efficiency while $BSNO_x$ was maintained.

One of the challenges encountered in optimizing fuel efficiency at lower power operating points was the need to maintain the exhaust throttle outlet temperature similar to that of the stock engine, while ensuring that $BSNO_x$ measurements remained within acceptable limits. At specific operating points such as 1900 rpm – 647 Nm and 2100 rpm – 580 Nm, the best fuel efficiency was achieved by increasing the exhaust throttle area and by increasing the EGRP speed. This combination effectively reduced engine delta pressure, thereby enhancing open-cycle efficiency. However, increasing the exhaust throttle area led to two different trade-offs: (1) the exhaust throttle outlet temperature decreased and (2) higher $BSNO_x$. To maintain $BSNO_x$ levels and improve the exhaust throttle outlet temperature, indexes with slightly more restricted exhaust throttle areas were chosen as the optimal points.

For the operating points above 1550 rpm lying on the torque curve, the best fuel efficiency, disregarding the pump's power consumption, was observed at pump speeds ranging from 7500 rpm to 10,000 rpm. These high pump speeds effectively reduced the engine delta pressure, resulting in improved open-cycle efficiency. However, the higher EGRP speeds led to increased power consumption by the pump. In real-life applications, this pump power would be connected to a 48V bus on a vehicle, reducing the total output power of the engine and resulting in a higher corrected BSFC.

Careful consideration was given to selecting the optimal index to achieve the highest possible fuel efficiency while still maintaining acceptable levels of $BSNO_x$. In Zar Nigar Ahmad's

Downloaded from SAE International by Purdue University Technical Papers, Wednesday, March 12, 2025

FIGURE 8 Actual pump speed of the best DOE operating points maintaining NO_x levels, and improving fuel economy.

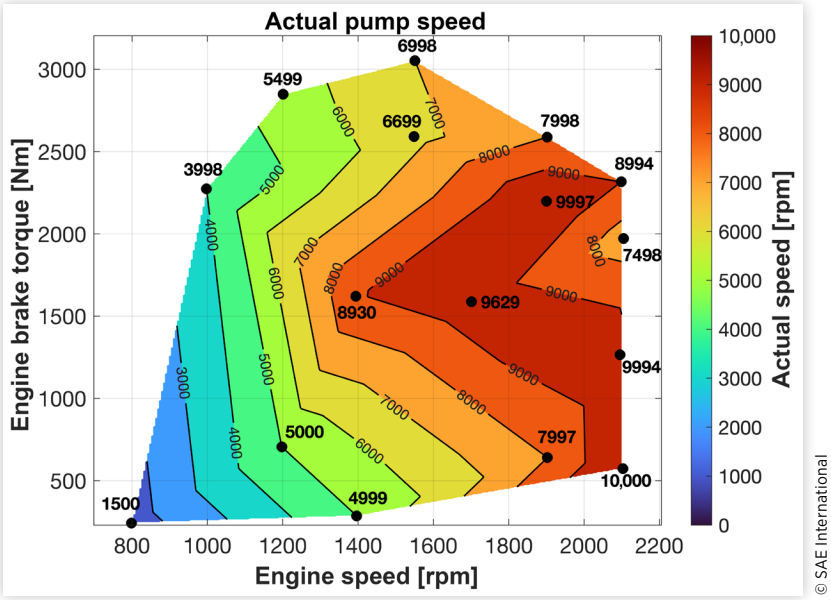

thesis [37] titled "Optimizing Fuel Economy and Emissions for Off-Road Diesel Engine Using Electric EGR Pump and High Efficiency Turbo," and Ahmad et al. [38] "Impact of Off-Road Engine Electrification through EGR Pumping on CO_2, Soot, and NO_x Emissions Reductions During Steady-State Operating Conditions," the control strategy used is described in greater detail along with all of the parameters analyzed determining the most optimal index.

Figures 8 and 9 display the pump speed and pump power for the DOE-optimized points. The best index from each operating point in the DOEs was utilized in creating a calibration map for steady-state testing and transient testing in closed loop. The indices chosen for the calibration had engine-out NO_x and engine-out PM below 25% of the stock engine performance, and engine-out temperatures similar to the stock engine performance. Other engine limits—including peak cylinder pressure, exhaust throttle outlet temperature—and other design constraints were maintained.

For BSFC calculations, the electrical energy from the EGRP was considered. When the pump was consuming power, the corrected power was calculated using Equation 1. A 90% electrical conversion efficiency was used for the pump.

FIGURE 9 Pump power of the best DOE operating points maintaining NO_x levels, and improving fuel economy.

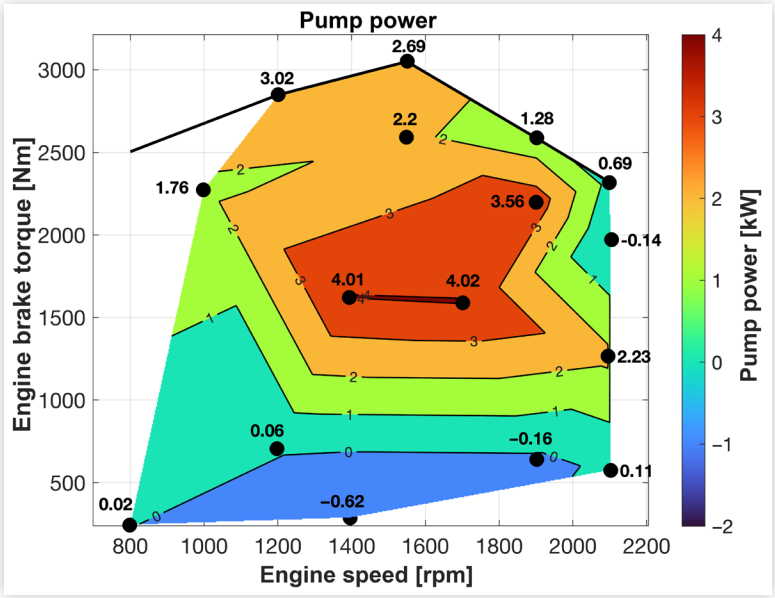

Downloaded from SAE International by Purdue University Technical Papers, Wednesday, March 12, 2025

FIGURE 10 Brake specific fuel consumption plot for steady state.

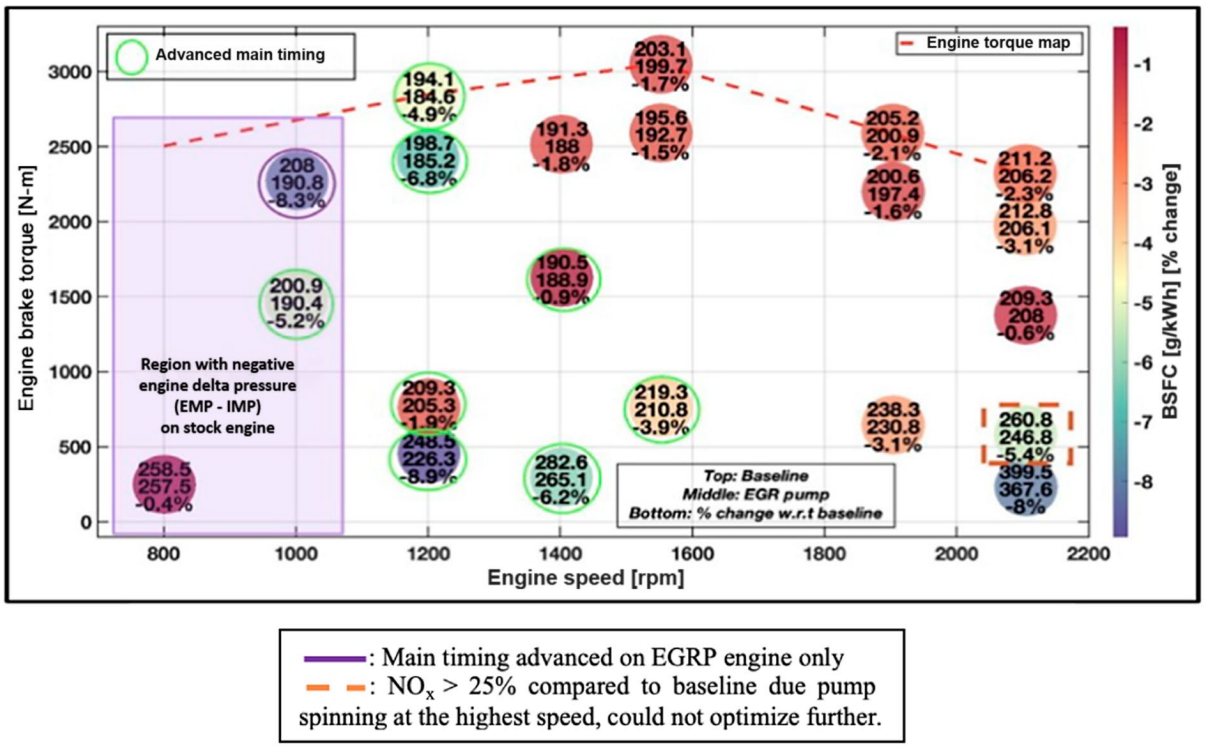
Advanced main timing
Engine torque map
Region with negative engine delta pressure (EMP - IMP) on stock engine
Top: Baseline
Middle: EGR pump
Bottom: % change w.r.t baseline
Engine brake torque [N-m]
Engine speed [rpm]
BSFC [g/kWh] [% change]
: Main timing advanced on EGRP engine only
: NOx > 25% compared to baseline due pump spinning at the highest speed, could not optimize further.

Reprinted with permission from Ref. [38]. © SAGE

$$\text{Power}_{\text{corrected}} = \text{Engine power} - \left(\frac{\text{Pump power}}{0.9}\right) \quad \text{Eq. (1)}$$

In the case of power generation by the pump, Equation 2 was used.

$$\text{Power}_{\text{corrected}} = \text{Engine power} - \left(\text{Pump power} \times 0.9\right) \quad \text{Eq. (2)}$$

The BSFC was determined by dividing the total fuel consumed by the engine's energy output, as shown in Equation 3.

$$\text{BSFC} = \left(\frac{\text{Fuel consumed}\left[\text{g}\right]}{\text{Energy}\left[\text{kWh}\right]}\right) \quad \text{Eq. (3)}$$

where

$$\text{Energy}\left[\text{kWh}\right] = \left(\frac{1}{3600\left[\text{s}\right]}\right) \int_{\text{start of cycle}}^{\text{end of cycle}} \text{Power}_{\text{corrected}}\, dt \quad \text{Eq. (4)}$$

In the stock configuration, the pump's power consumption was zero because the EGRP was not incorporated into the setup. The cycle energy for the stock engine was determined by integrating the engine power.

A comprehensive analysis of steady-state results was conducted by Zar Nigar Ahmad in her thesis [37], and also explained in Ahmad et al. [38]. These works provide a detailed explanation on the steady-state DOE strategy used, the resulting calibration map, and the steady-state characterization of the engine, with the same EGRP and high-efficiency turbocharger. Hence, this article does not describe the detailed effort to calibrate the engine operation. However, the BSFC, BSNO$_x$, and BSPM results from the steady-state testing are presented in Figures 10, 11, and 12, respectively. Further information about this is discussed in-depth in the work of Ahmad et al. [38].

Results

The initial optimized calibration map was slightly modified for mid–high engine speeds at low engine loads to increase the pressure ratio across the pump. This improved the motor's capability to maintain the commanded pump speed and function accordingly. With these modifications the NRTC, LLAC, CSLA tests, and RMC were performed.

The NRTC and CSLA tests were each performed twice to ensure consistency and repeatability since the NRTC is utilized in the U.S. EPA Tier 4 regulations, and the CSLA is crucial for determining time response. Repeatability was seen among the NRTC and with the CSLA test for time response. An additional measure was implemented to verify consistent results. After each cycle, a repeat point was executed to confirm that boundary conditions were maintained and to ensure the reliability of the presented data.

Downloaded from SAE International by Purdue University Technical Papers, Wednesday, March 12, 2025

FIGURE 11 Brake specific nitrogen oxide plot for steady state.

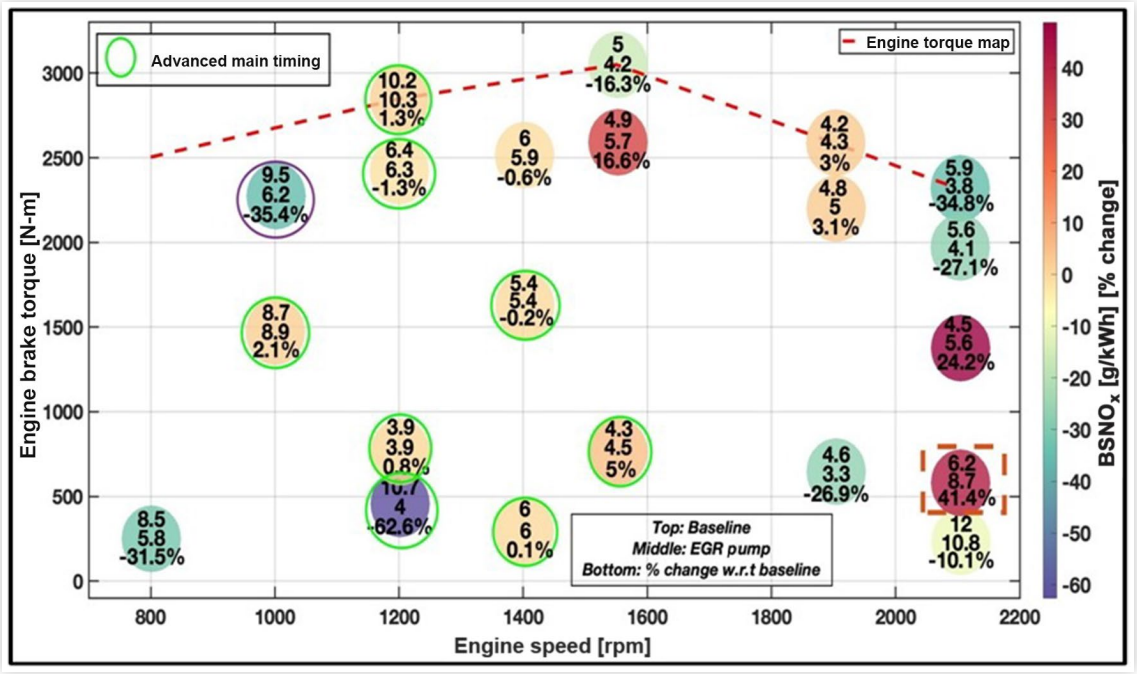

Reprinted with permission from Ref. [38]. © SAGE

FIGURE 12 Brake specific particulate matter plot for steady state.

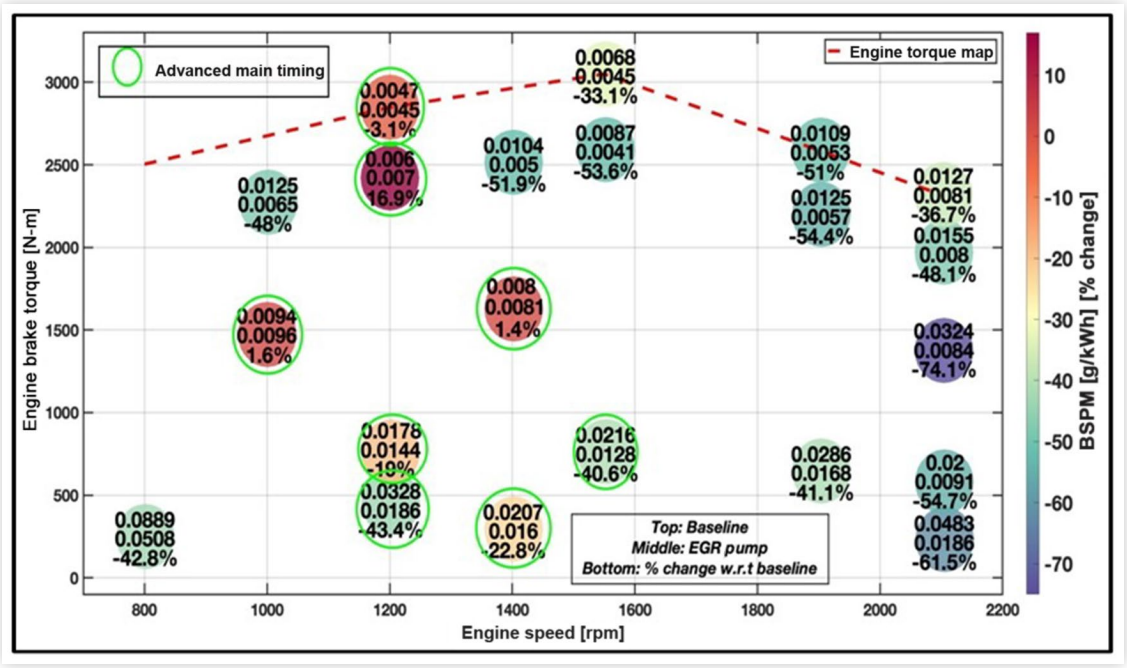

Reprinted with permission from Ref. [38]. © SAGE

Downloaded from SAE International by Purdue University Technical Papers, Wednesday, March 12, 2025

TABLE 5 Uncertainty of key parameters at repeat point.

Measured parameters	Uncertainty
Speed (rpm)	±0.11%
Torque (Nm)	±0.1%
Air flow rate (kg/h)	±0.5%
Diesel flow rate (kg/h)	±0.06%
Engine-out exhaust temperature (°C)	±0.34%
Nitric oxide (g/kWh)	±1.75%
PM	±6.95%

© SAE International

Using 12 repeat point data collected over a period of 2 weeks, the typical uncertainty values for key measured parameters were calculated, and presented in Table 5. This follows the method described in the work of Starnes et al. [39], with 95% confidence and $\pm 2\sigma$ limits using the t-distribution.

To compare the stock turbocharger to the high-efficiency turbocharger, using Equation 5, the efficiency of both turbochargers was calculated. The method explained in "CIMAC's 'Turbocharging Efficiencies—Definitions and Guidelines for Measurement and Calculation'" [40] was used. Figure 13 displays a segment of the high-pressure turbochargers' efficiency for both configurations during the NRTC transient test, showing performance across low to high speeds with high torque. Since the goal of a turbocharger is to enhance engine power, its efficiency at operating points with high torque is important. In this section, the efficiency of the high-efficiency turbocharger (in red) is consistently higher than the stock turbocharger.

$$\eta_{TC} = \frac{\dot{m}_{air} C_{p,air} T_{Ci} \left[\left(\frac{P_{Co}}{P_{Ci}} \right)^{\frac{\gamma_a - 1}{\gamma_a}} - 1 \right]}{\dot{m}_{exh} C_{p,exh} T_{T_i} \left[1 - \left(\frac{P_{To}}{P_{Ti}} \right)^{\frac{1-\gamma_{exh}}{\gamma_{exh}}} \right]} \quad \text{Eq. (5)}$$

where $\dot{m}_{air}$ is the fresh air flow rate, $\dot{m}_{fuel}$ is the fuel flow rate, $C_{p,air}$ is the specific heat constant of fresh air, $C_{p,exh}$ is the specific heat constant of exhaust gas, T_{Ci} is the low-pressure compressor inlet temperature, T_{Co} is the high-pressure compressor outlet temperature, P_{Ti} is the high-pressure turbine inlet pressure, P_{To} is the low-pressure turbine outlet pressure, P_{Ci} is the low-pressure compressor inlet pressure, P_{Co} is the high-pressure compressor outlet pressure, η_{TC} is the overall turbocharger efficiency, γ_a is the specific heat of air, γ_{exh} is the specific heat of exhaust gas.

Nonroad Transient Cycle

The hot NRTC was executed on both the stock engine and the EGRP-equipped engine, but with the EGRP and high-efficiency turbocharger configuration not all of the desired torque setpoints were achieved. The green segments represented in Figure 14 highlight instances where the EGRP configuration did not match the baseline engine load. To assess the differences among the reference cycle, the baseline NRTC, and the EGRP NRTC, three distinct regions were magnified in Figure 14. As a result, not all the statistical criteria required to validate the NRTC duty cycle under the U.S. EPA Tier 4 emission standards were met.

FIGURE 13 Comparison between the efficiency of stock turbocharger and high-efficiency turbocharger at high engine speed–load section of NRTC.

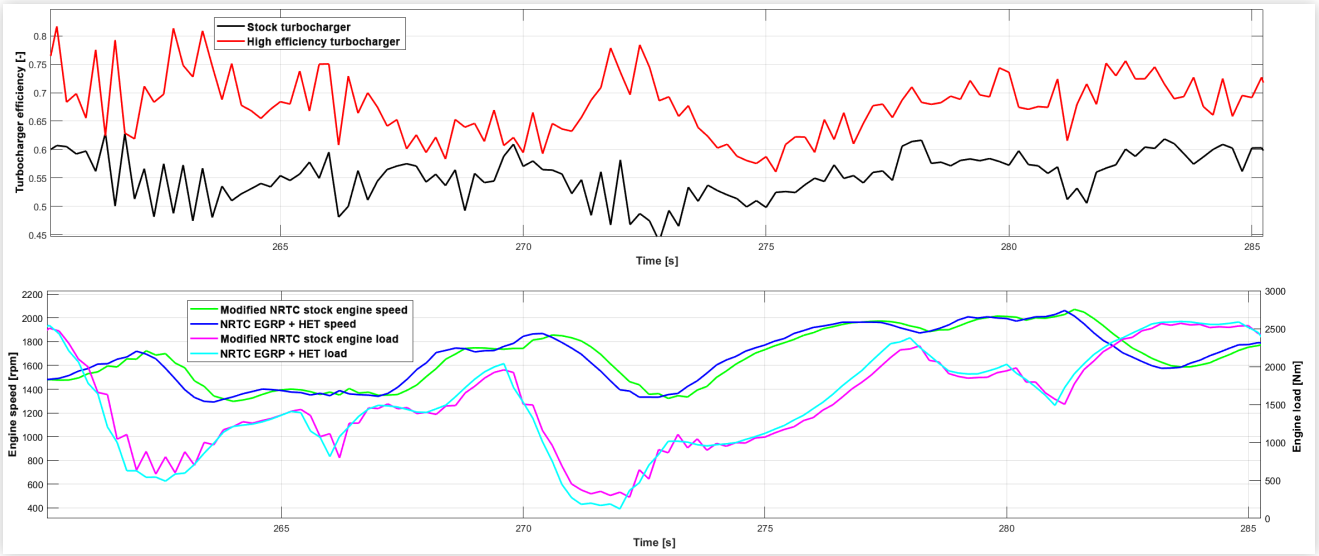

© SAE International

Downloaded from SAE International by Purdue University Technical Papers, Wednesday, March 12, 2025

FIGURE 14 Comparison of engine load between the EGRP and high-efficiency turbocharger engine vs. the baseline engine.

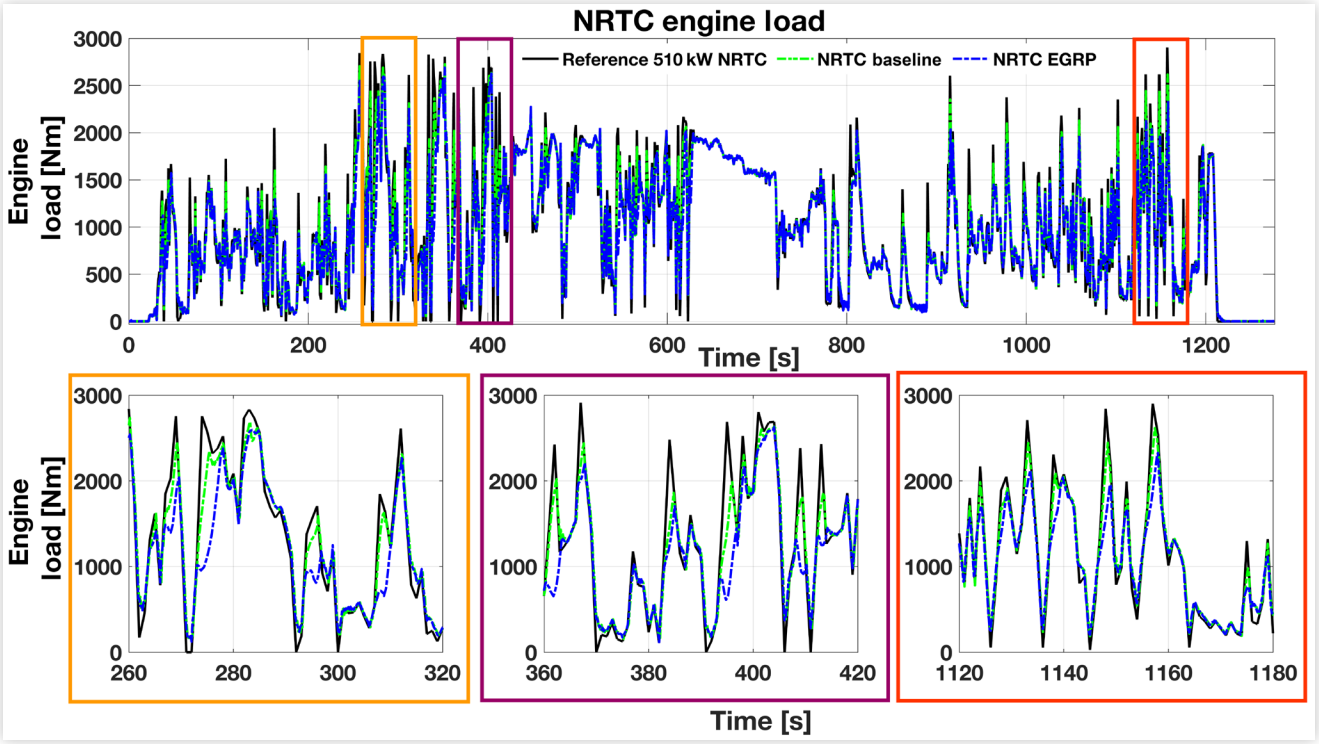

© SAE International

The EGRP-equipped engine's inability to meet the reference torque values is due to insufficient fresh airflow. In Figure 15, regions where the engine fell short of reaching the reference torque setpoints are highlighted by orange circles. An analysis between the commanded speed and the actual pump speed was conducted. In Figure 15, the commanded pump speed (blue) signifies the speed requested by the ECU, while the actual pump speed (red) reflects the pump's operational speed. Orange arrows indicate the regions where the actual pump speed exceeded the commanded pump speed. In this figure, the actual pump speed decelerates at approximately 2000 rpm/s. This ramp rate is attributed to the motor controller software protecting the motor from electrical and mechanical overstress. Unfortunately, this ramp rate permits more EGR than intended, displacing the fresh air required to produce torque. The baseline EGR valve position (magenta) is also plotted in Figure 15. In regions indicated by the orange arrow, the EGR valve is shut, blocking exhaust gas from entering the intake manifold. Without EGR, the stock engine achieves higher torque values compared to the engine equipped with the EGRP and high-efficiency turbocharger.

The total cycle work calculated from the NRTC baseline was 64.8 kWh. Factoring in the pump power, the cycle work from the first and second runs with the EGRP-equipped engine was 62.3 kWh and 62.4 kWh, resulting in a 3.9% and 3.7% reduction in cycle work from the stock engine. Without taking into account the pump power, the cycle work was 62.7 kWh and 62.8 kWh, accounting for a 3.2% and 3.1% reduction in cycle work compared to the stock engine, as indicated in Table 6.

The 3 kW continuous power rating of the EGRP did contribute to the loss of cycle work. The motor did not have the power to retard the torque required to maintain the commanded pump speed, so the pump dropped speed linearly to safeguard the motor. The motor controller software included a ramp rate to protect the motor. Due to the lack of fresh airflow with the EGRP-equipped engine, the engine ECU was hitting the smoke map limit, necessitating a reduction in fueling. The smoke map limit is modeled within the ECU to reduce fueling when there is insufficient fresh air flow, ensuring there is no excessive soot generation. This led to a reduction in cycle work.

To accurately evaluate the new technology, the measured engine speed and measured engine torque from the engine with the EGRP and high-efficiency turbocharger were utilized to develop a modified NRTC pattern to run on the stock engine. This helps to ensure that there is a direct and fair comparison between both configurations. Also, the electrical energy of the electric motor in the EGRP is accounted for in the fuel consumption calculations. With the EGRP and high-efficiency turbocharger configuration, there was a 1.3% improvement in BSFC and a 33.1% improvement in BSPM compared to the modified NRTC on the stock engine. However, there was a 12.9% increase in $BSNO_x$. These results can be observed in Table 7.

Improvements in BSFC may be attributed to the improvement in open-cycle efficiency. In Figure 16, the blue circles represent all the collected operating points in the modified NRTC at 5 Hz sampling frequency. The light blue-shaded regions highlight improvements in BSFC and brake thermal

Downloaded from SAE International by Purdue University Technical Papers, Wednesday, March 12, 2025

FIGURE 15 Top: The comparison of engine load between the different configurations from 540 s to 650 s in the NRTC. Bottom: The commanded and actual pump speed of the EGRP plotted with the baseline EGR valve from 540 s to 650 s in the NRTC.

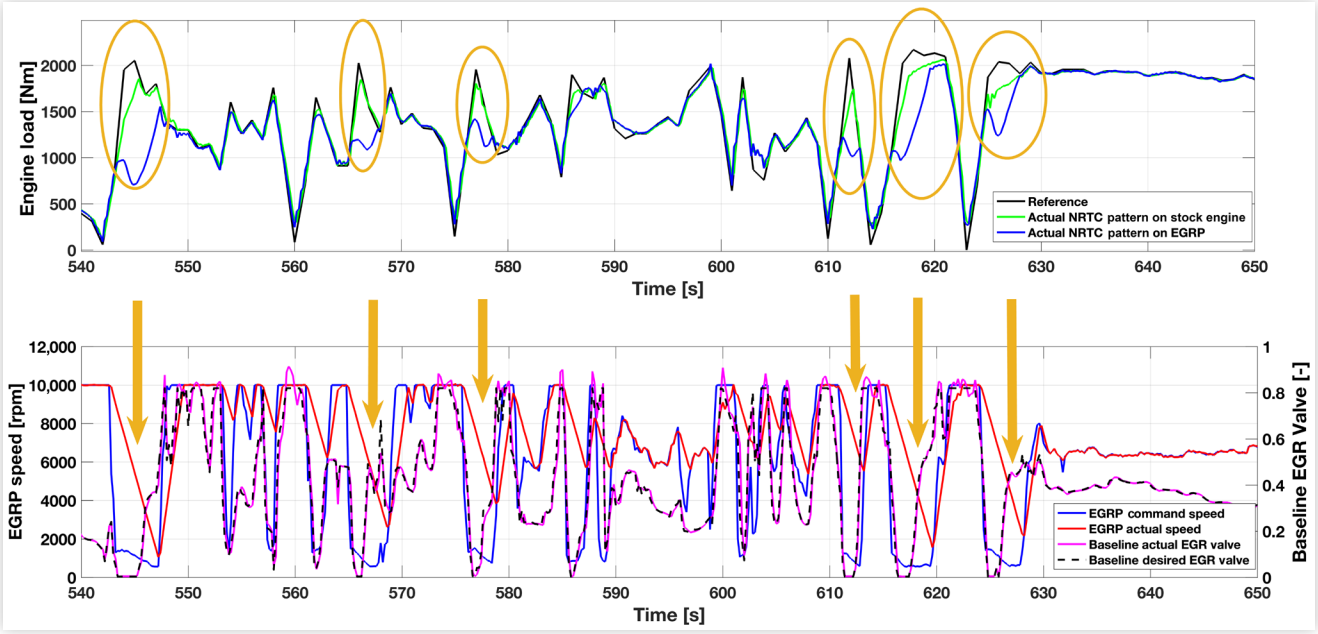

© SAE International

efficiency due to an improvement in open-cycle efficiency determined in steady-state testing [37]. Although the engine spends a considerable amount of time at near-idle and lighter load conditions, as indicated in Figure 16, these are not locations where the EGRP technology was used to attempt to improve fuel efficiency. Therefore, this study did not focus on conditions at idle. The green-shaded region indicates where open and closed-cycle efficiency improved the brake thermal efficiency and BSFC. No operating points were within the green-shaded region, suggesting that the BSFC improvement is projected to come from improved open-cycle efficiency.

Low Load Application Cycle

In the LLAC, the engine with the EGRP and high-efficiency turbocharger also undershoots torque set points due to insufficient fresh airflow.

TABLE 6 Results of the NRTC.

Classified run	Cycle work g/kWh	BSFC g/kWh	Engine-out $BSNO_x$ g/kWh	Engine-out BSPM g/kWh
NRTC baseline	64.8	214.8	4.86	0.0232
NRTC baseline	64.8	216.9	4.83	0.0283
NRTC EGRP + HET	62.3*	212.6*	5.08*	0.0195*
NRTC EGRP + HET	62.4*	213.3*	5.08*	0.0200*
Modified NRTC	63.0	216.1	4.50	0.0299
Modified NRTC	62.8	215.8	4.50	N/A

* Accounting for pump power

© SAE International

The cycle work of the stock engine was 106.9 kWh. For the EGRP-equipped engine, the cycle work was 105.8 kWh without accounting for the pump power and 105.2 kWh when accounting for the pump power.

Although the percentage change of cycle work between the stock engine and EGRP-equipped engine was below 2%, to ensure fair comparisons between the EGRP-equipped engine and the stock engine, a modified LLAC was developed. Like the modified NRTC, the measured engine speed and engine load from the LLAC with the EGRP and high-efficiency turbocharger were used to construct the modified LLAC. The modified LLAC was run on the stock engine. The results from the LLAC baseline, the LLAC with the EGRP and

TABLE 7 Percentage difference between modified NRTC cycle on stock engine and the engine with high-efficiency turbocharger and EGRP.

	NRTC EGRP + HET	Modified NRTC	Percentage difference (%)
Drive shaft energy (kWh)	62.8	63.0	
Pump energy (kWh)	0.4	0	
Output energy (kWh)	62.4*	63.0	
Fuel consumed (g)	13,321.6	13,616.6	
BSFC (g/kWh)	213.3*	216.1	**1.3%**
$BSNO_x$ (g/kWh)	5.08*	4.50	**12.9%**
BSPM (g/kWh)	0.0200*	0.0299	**33.1%**

Pump energy—Energy consumed by the pump
Drive shaft energy—Energy converted from the drive shaft
Output energy = Drive shaft energy – Pump power
* Accounting for pump power

© SAE International

Downloaded from SAE International by Purdue University Technical Papers, Wednesday, March 12, 2025

FIGURE 16 Improvement in BSFC for the NRTC can be attributed to enhanced open-cycle efficiency at lower engine torques, shaded in light blue, identified from steady-state testing.

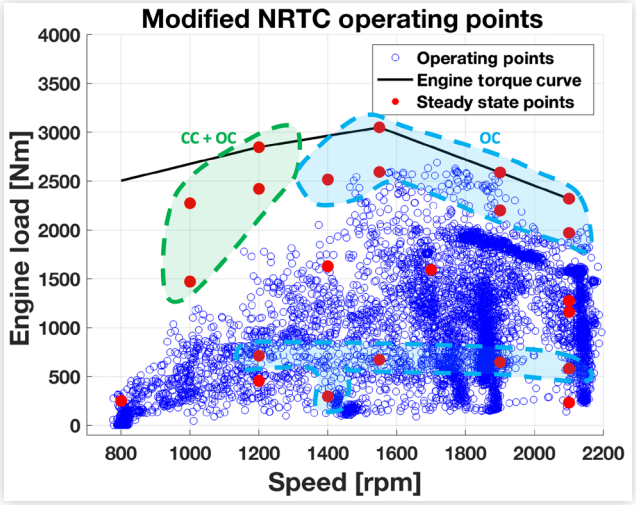

© SAE International

FIGURE 17 Modified LLAC operating points lying within the light blue-shaded region suggests improved open-cycle efficiency.

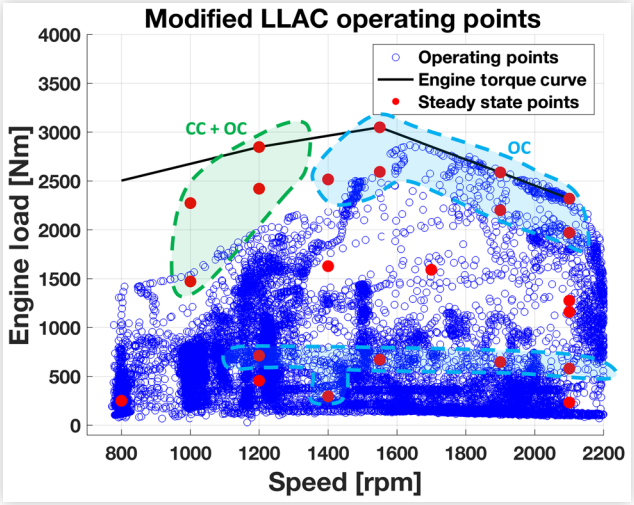

© SAE International

high-efficiency turbocharger, and the modified LLAC on the stock engine are shown in Table 8.

After comparing the results of the modified LLAC on the stock engine to the LLAC with the EGRP and high-efficiency turbocharger, a 2.5% improvement in BSFC and an 11.1% improvement in $BSNO_x$ were observed. The BSPM increased by 34.2%, as shown in Table 9.

Similar to the modified NRTC, operating points from the modified LLAC are located within the area where enhanced open-cycle efficiency improved both BSFC and brake thermal efficiency, as depicted in Figure 17.

Given that the modified LLAC primarily operates at low loads, the exhaust throttle outlet temperature was analyzed for both configurations to ensure the exhaust throttle outlet temperature was above 250°C for adequate thermal management. Figure 18 shows the EGRP and high-efficiency turbocharger remain above 250°C for the majority of the cycle.

In the modified LLAC stock configuration, a discernible drop in exhaust throttle outlet temperature is observed in regions where the torque is sustained below 220 Nm, including 1120 s to 1378 s, 3075 s to 3420 s, and from 3700 s to 4045 s. During these intervals, the exhaust mass flow rate is higher for the stock engine. This difference in exhaust mass flow rate is attributed to the exhaust throttle area being fully open on the stock engine, but nearly closed with the EGRP configuration.

TABLE 8 LLAC results.

Classified run	Cycle work (kWh)	BSFC (g/kWh)	Engine-out $BSNO_x$ (g/kWh)	Engine-out BSPM (g/kWh)
LLAC baseline	106.9	236.8	6.54	0.0182
LLAC EGRP + HET	105.2*	230.5*	5.67*	0.0255*
Modified LLAC	105.4	236.5	6.38	0.0190

* Accounting for pump power

© SAE International

CSLA Test

The CSLA test was performed on six different operating points listed in Table 10 two separate times with both the stock and EGRP configurations.

The engine equipped with the EGRP and high-efficiency turbocharger demonstrated slower response times to reach 90% load compared to the stock engine during the CSLA tests. Figure 19 provides a comparison of the average response time to 90% load for both the baseline and EGRP configuration, revealing disparities ranging from 0.1 s at 800 rpm to 1.6 s at 1900 rpm.

TABLE 9 Percentage difference between modified LLAC cycle on stock engine and the engine with high-efficiency turbocharger and EGRP.

	LLAC EGRP + HET	Modified LLAC	Percentage difference (%)
Drive shaft energy (kWh)	105.8	105.4	
Pump energy (kWh)	0.5	0	
Output energy (kWh)	105.2*	105.4	
Fuel consumed (g)	24,256.2	24,923.2	
BSFC (g/kWh)	230.5*	236.5	**2.5%**
$BSNO_x$ (g/kWh)	5.67*	6.38	**11.1%**
BSPM (g/kWh)	0.0255*	0.0190	**34.2%**

Pump energy—Energy consumed by the pump
Drive shaft energy—Energy converted from the drive shaft
Output energy = Drive shaft energy – Pump power
* Accounting for pump power

© SAE International

Downloaded from SAE International by Purdue University Technical Papers, Wednesday, March 12, 2025

FIGURE 18 The exhaust throttle outlet temperature primarily stays above 250°C for the EGRP-equipped engine.

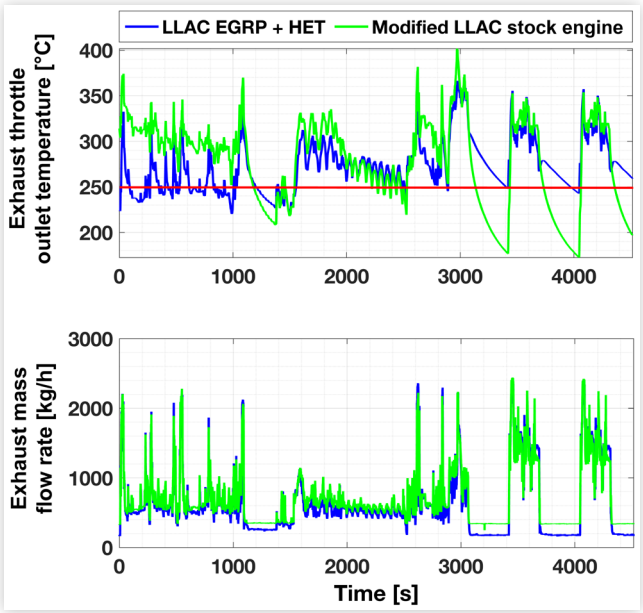

© SAE International

Figure 20 overlays both configurations at the point of the throttle snap for the 1900 rpm operating point. The difference in time response is evident by the EGRP-equipped engine load (green) deviating from the baseline engine load (black). During the transient response, the EGR valve on the stock engine closes, preventing exhaust gases from entering the intake manifold. However, with the EGRP configuration, the actual pump speed decelerates at approximately 2000 rpm/s during the transient response, leading to more exhaust gas recirculation than intended. In the EGRP configuration, the EGR valve remains fully open during the transient responses, so the pump speed is the only way to reduce EGR flow. As a result, the engine experiences a slower time response to reach 90% load. This pattern was consistent across all operating points except the 800 rpm operating point.

Figure 21 displays the average peak soot measurement for both configurations. The EGRP configuration shows significantly lower peak soot measurements at operating points of 800 rpm, 1000 rpm, and 1200 rpm compared to the baseline configuration. This could be due to the advancement in main timing with the EGRP configuration, a more complete combustion process with the additional time to reach load, less fuel being injected at the start of the throttle snap, or a combination of the different factors mentioned. For the remaining 1550 rpm, 1900 rpm, and 2100 rpm operating points, the EGRP and high-efficiency turbocharger setup displayed higher peak soot measurements compared to the baseline setup. The slower changes in EGRP speed during transients caused higher soot emissions at elevated speeds, since EGR flow was higher than desired, as indicated in Figure 20.

TABLE 10 List of CSLA operating points executed in this study.

CSLA operating points
800 rpm – 2504 Nm
1000 rpm – 2275 Nm
1200 rpm – 2848 Nm
1550 rpm – 3050 Nm
1900 rpm – 2588 Nm
2100 rpm – 2319 Nm

© SAE International

FIGURE 19 The average time response to 90% load for the CSLA tests.

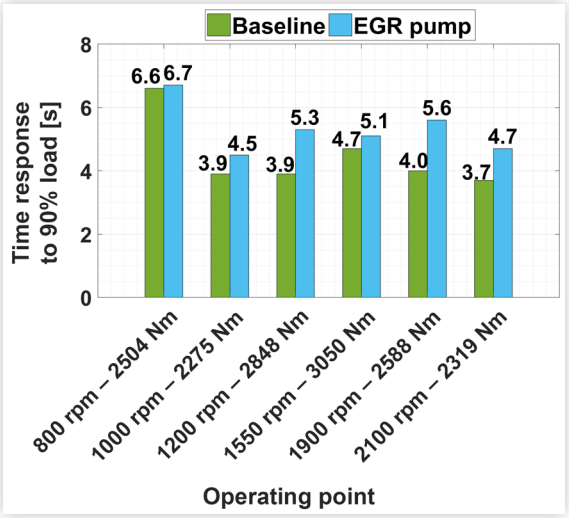

© SAE International

RMC

To stay below the advertised dynamometer limits, the RMC cycle was modified from a maximum power of 510 kW to 500 kW. Table 11 compares the RMC baseline results to the RMC EGRP and high-efficiency turbocharger results.

FIGURE 20 Comparison of the 1900 rpm CSLA test between the stock hardware configuration and the EGRP and high-efficiency turbocharger configuration.

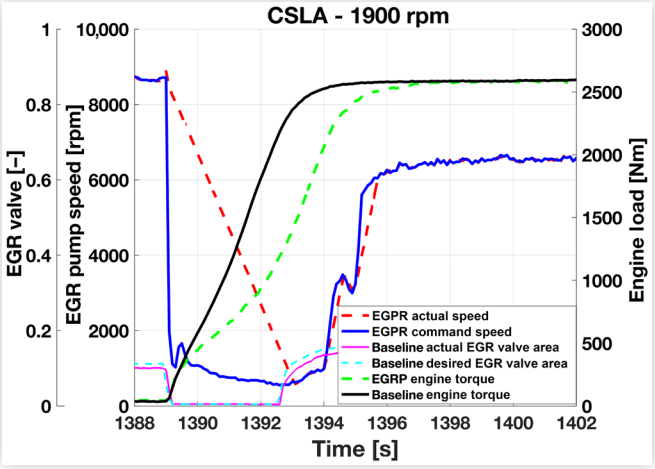

© SAE International

Downloaded from SAE International by Purdue University Technical Papers, Wednesday, March 12, 2025

FIGURE 21 Average peak soot measurements for the CSLA tests.

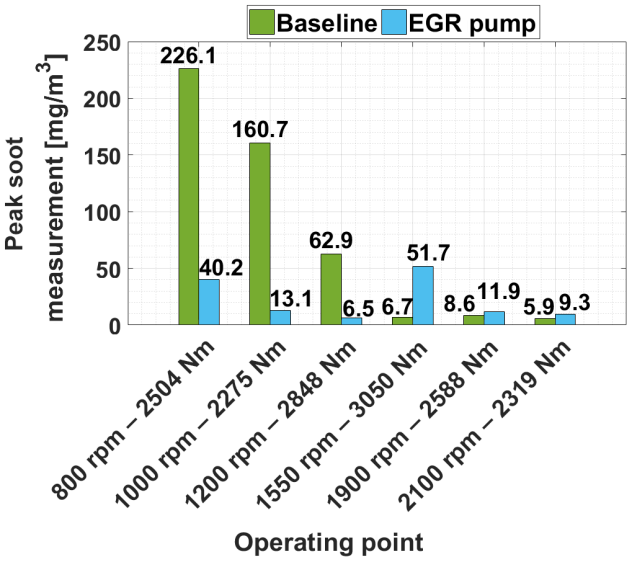

© SAE International

Overall, a 1.3% improvement in BSFC was observed with the EGRP and high-efficiency turbocharger. The increase in $BSNO_x$ was merely 2.8% as can be seen in Table 12.

BSFC and engine-out $BSNO_x$ were calculated for the operating points at intermediate speeds and rated speeds in the RMC. The percentage change in BSFC and $BSNO_x$ between the EGRP-equipped engine and the stock engine for the seven different operating points is displayed in Figures 22 and 23. The negative sign represents an improvement in BSFC and a reduction in $BSNO_x$. PM data was not collected during the RMC test. However, since the RMC is a relatively slow transient representation of the steady-state operating points, the steady-state data in Figure 12 provides a rough estimate of the expected BSPM values for RMC.

Conclusion and Future Work

The primary focus of this study was to compare the fuel efficiency and engine-out emissions of the EGRP-equipped engine with the stock engine for various drive cycles including the NRTC, LLAC, and RMC and to evaluate the time response to 90% load for the CSLA tests between both configurations. This study specifically demonstrates the shortcomings and benefits of the prototype EGRP, when paired with a high-efficiency turbocharger, in an off-road diesel engine.

TABLE 11 RMC results.

Classified run	Cycle work (kWh)	BSFC (g/kWh)	Engine-out $BSNO_x$ (g/kWh)
RMC baseline	141.0	208.8	5.28
RMC EGRP+ HET	141.0*	206.1*	5.43*

* Accounting for pump power

© SAE International

TABLE 12 Percentage difference between RMC cycle on stock engine and the engine with high-efficiency turbocharger and EGRP.

	RMC EGRP + HET	RMC stock	Percentage difference (%)
Drive shaft energy (kWh)	141.2	141.0	
Pump energy (kWh)	0.2	0	
Output energy (kWh)	141.0*	141.0	
Fuel consumed (g)	29,056.9	29,102.6	
BSFC (g/kWh)	206.1*	208.8	**1.3%**
$BSNO_x$ (g/kWh)	5.43*	5.28	**2.8%**

Pump energy—Energy consumed by the pump
Drive shaft energy—Energy converted from the drive shaft
Output energy = Drive shaft energy – Pump power
* Accounting for pump power

© SAE International

During NRTC, LLAC, and CSLA testing with the EGRP and high-efficiency turbocharger configuration, the setup was unable to produce the required torque due to shortcomings of the EGRP. A modified version of the NRTC and LLAC was developed and run on the stock engine to accurately compare engine performance between the engine with the EGRP and high-efficiency turbocharger and the stock engine. For the modified NRTC, a 1.3% improvement in BSFC was seen with the EGRP and high-efficiency turbocharger hardware. Whereas for the modified LLAC a 2.5% improvement in BSFC was observed with the EGRP and high-efficiency turbocharger hardware. The RMC, requiring no modifications because of the EGRP, showed a 1.3% improvement in BSFC.

FIGURE 22 Percent change in BSFC comparing the EGRP-equipped engine with stock engine.

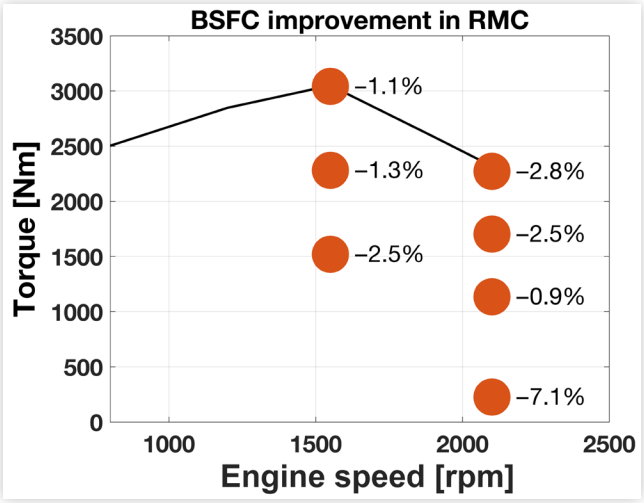

© SAE International

Downloaded from SAE International by Purdue University Technical Papers, Wednesday, March 12, 2025

FIGURE 23 Percent change in engine-out $BSNO_x$ comparing the EGRP-equipped engine with stock engine.

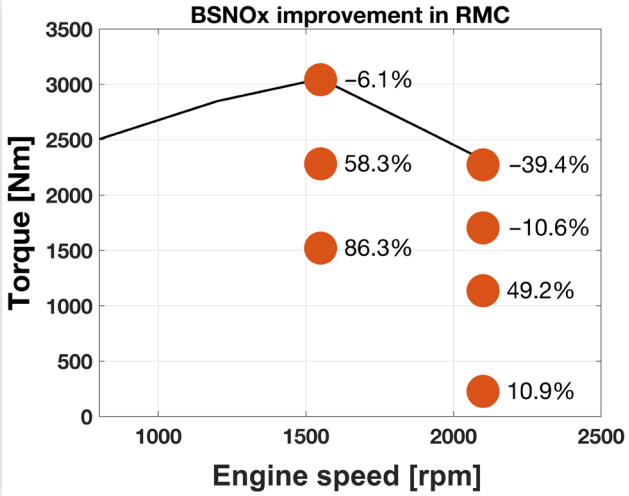

© SAE International

Overall, the results of this study show that implementing the EGRP and high-efficiency turbocharger improves BSFC at similar NO_x levels. However, while the impact is meaningfully advantageous, it was limited by the EGRP design constraints, which were EGRP speed and power. The requirement to deliver adequate airflow in the cylinder was not met due to excess EGR. Higher EGR flow results in lower airflow. This study does not focus on resolving this issue, but demonstrates benefits and limitations of the EGRP. Future efforts should address this shortcoming.

Examining the fuel benefits of the NRTC and LLAC with a higher-power motor would provide valuable insights. With a higher-power motor, the deceleration ramp rate would be increased, facilitating sufficient fresh airflow for the engine to produce torque. Hence, it would be advantageous to develop an EGRP with a more powerful electric motor that is able to accelerate and decelerate the EGRP more quickly. An alternative approach could include refining the control logic to have the EGR valve vary positions with the EGRP and high-efficiency turbocharger hardware. This would restrict the amount of exhaust gas recirculating back into the engine.

Off-road engines are critical for everyday use in various industries. Exploring innovative technologies to reduce emissions and improve fuel economy helps economically and environmentally. This study shows that the EGRP has the potential to reduce emissions and improve fuel economy on off-road diesel engines. However, to meet future emissions regulations using the EGRP, the automotive industry must address concerns such as the lack of fresh airflow. This can be achieved by designing an EGRP with a high-power motor or by modifying the control strategy to adjust EGR valve positions with the EGRP, ensuring the EGR valve is not completely open. Once the shortcomings are addressed, the authors anticipate fuel savings for the original regulatory drive cycles. Also, future studies can focus on exploring the long-term durability of EGR systems and turbochargers in off-road diesel engines.

Acknowledgements

The authors would like to express gratitude and appreciation to the Herrick engineering technicians, Frank Lee and Jose Lopez Romero, for their support and assistance. The authors also wish to thank Lakshmi Prasad, Nathanial Bergland, and David Arntz from John Deere, as well as Nam Do, Michael Ellinger, and Jim Malone from Eaton, for their guidance and contributions.

Contact Information

Gregory Shaver, corresponding author
gshaver@purdue.edu

References

1. Stanton, D.W., "Systematic Development of Highly Efficient and Clean Engines to Meet Future Commercial Vehicle Greenhouse Gas Regulations," *SAE Int. J. Engines* 6, no. 3 (2013): 1395-1480, doi:https://doi.org/10.4271/2013-01-2421.
2. McCaffery, C., Yang, J., Karavalakis, G., Yoon, S. et al., "Evaluation of Small Off-Road Diesel Engine Emissions and Aftertreatment Systems," *Energy* 251 (2022): 123903.
3. Arden Pope, C. III and Dockery, D.W., "Health Effects of Fine Particulate Air Pollution: Lines That Connect," *Journal of the Air & Waste Management Association* 56, no. 6 (2006): 709-742.
4. Agency for Toxic Substances and Disease Registry, "ToxFAQs™ for Nitrogen Oxides," 2014, accessed May 13, 2024, https://wwwn.cdc.gov/TSP/ToxFAQs/ToxFAQsDetails.aspx?faqid=396&toxid=69.
5. Lammel, G. and GraBl, H., "Greenhouse Effect of NO_x," *Environmental Science and Pollution Research* 2 (1995): 40-45.
6. United States Environmental Protection Agency, "Air Pollutant Emissions Trends Data," 2024, accessed May 13, 2024, https://www.epa.gov/air-emissions-inventories/air-pollutant-emissions-trends-data.
7. California Air Resources Board, "Tier 5 Rulemaking Workshop II: Proposed Emission Standards," 2021, accessed March 03, 2024, https://ww2.arb.ca.gov/sites/default/files/2023-10/%232%20Proposed%20Emission%20Standards-ADA-10232023-revised.pdf.
8. Xin, Q., *Diesel Engine System Design* (Elsevier, Woodhead Publishing, Cambridge, UK, 2011)
9. Agarwal, D., Singh, S.K., and Agarwal, A.K., "Effect of Exhaust Gas Recirculation (EGR) on Performance, Emissions, Deposits and Durability of a Constant Speed Compression Ignition Engine," *Applied Energy* 88, no. 8 (2011): 2900-2907.
10. Bagal, N.L. and Bhardwaj, D., "48V EGR Pump System Development and Fuel Benefit Evaluation," *Frontiers in Mechanical Engineering* 8 (2022): 673134.

Downloaded from SAE International by Purdue University Technical Papers, Wednesday, March 12, 2025

11. Johnson, G., Bockstanz, B., Bagal, N., Hopkins, J. et al., "48V Exhaust Gas Recirculation Pump: Reducing Carbon Dioxide with High-Efficiency Turbochargers without Increasing Engine-Out NOx," *SAE Int. J. Commer. Veh.* 14, no. 3 (2021): 303-309, doi:https://doi.org/10.4271/02-14-03-0024.
12. Eaton Corporation, "EGR Pump Prototype Installation Guide," 2020.
13. Darcovich, K., Ribberink, H., Qiu, K., and Soufflet, E., "Battery Pack Prospects for Long-Haul Transport Trucks Considering Electrified Highways and Megawatt Charging," *World Electric Vehicle Journal* 14, no. 3 (2023): 60.
14. Beltrami, D., Iora, P., Tribioli, L., and Uberti, S., "Electrification of Compact Off-Highway Vehicles—Overview of the Current State of the Art and Trends," *Energies* 14, no. 17 (2021): 5565.
15. Qiu, W., Ashta, S., Shaver, G.M., Mazanec, J. et al., "System Configuration, Control Development, and In-Field Validation of a Hybrid Electric Wheel Loader Featuring Electrically-Boosted Engine," *Control Engineering Practice* 150 (2024): 105989.
16. Thomasson, A., Eriksson, L., Leufven, O., and Andersson, P., "Wastegate Actuator Modeling and Model-Based Boost Pressure Control," *IFAC Proceedings Volumes* 42, no. 26 (2009): 87-94.
17. Deere, J., "JD14 Engine," Brochure, accessed February 24, 2024, https://johndeere.widen.net/s/8lbhpctn2v/jdpsmaster--dswt158-jd14-engine-flyer.
18. U.S. Environmental Protection Agency, "Control of Emissions of Air Pollution from Nonroad Diesel Engines and Fuel," *Federal Register* 69 (2004): 39253-39259.
19. California Air Resources Board, "Analyzing Real-World Engine Duty Cycles of Construction Equipment and Assessing the Need for a Low Load Cycles," 2021, accessed March 03, 2024, https://ww2.arb.ca.gov/sites/default/files/classic//msprog/tier5/low_load_cycle.pdf.
20. United Nations, "Addendum 95: Regulation No. 96 Revision 3," 2014.
21. United States Environmental Protection Agency, "EPA Nonregulatory Nonroad Duty Cycles," 2023, accessed May 3, 2024, https://www.epa.gov/moves/epa-nonregulatory-nonroad-duty-cycles.
22. Samulski, M.J. and Jackson, C.C., "Effects of Steady-State and Transient Operation on Exhaust Emissions from Nonroad and Highway Diesel Engines," *SAE Transactions* 107 (1998): 2068-2080.
23. Lindgren, M., "A Transient Fuel Consumption Model for Non-road Mobile Machinery," *Biosystems Engineering* 91, no. 2 (2005): 139-147.
24. United States Environmental Protection Agency, "Final Regulatory Analysis: Control of Emissions from Nonroad Diesel Engines," Technical Report, 2004.
25. Giakoumis, E.G., *Driving and Engine Cycles*. Vol. 1 (Cham, Switzerland: Springer, 2017)
26. Lee, K., Lee, J., Lee, S., Kwangchul, O. et al., "Fuel Consumption and Emission Reduction for Non-Road Diesel Engines with Electrically Heated Catalysts," *Catalysts* 13, no. 6 (2023): 950.
27. Di Luca, G., Muccillo, M., Giardiello, G., Gimelli, A. et al., "1D and Map-Based Modeling Approaches for Railway Compression Ignition Engine in NRTC Application," *Applied Sciences* 12, no. 5 (2022): 2665.
28. Wang, T.J., Kim, D.S., and Ahn, T.S., "Simulation Study on Improving the Selective Catalytic Reduction Efficiency by Using the Temperature Rise in a Non-Road Transient Cycle," *Proceedings of the Institution of Mechanical Engineers, Part D: Journal of Automobile Engineering* 231, no. 6 (2017): 810-827.
29. Sharp, C.A., "Off-Road Diesel Low-Emission Demo for Nitrogen Oxides (NOx), Particulate Matter (PM), and Toxics," Technical Report, Southwest Research Institute, 2021.
30. Protection of Environment, 40 C.F.R. § 1065, 2020.
31. Gu, W. and Su, W., "Study on the Effect of Exhaust Gas Recirculation Coupled Variable Geometry Turbocharger and Fuel Quantity Control on Transient Performance of Turbocharged Diesel Engine," *Energies* 16, no. 16 (2023): 6008.
32. Liu, Y., Song, Y., Leng, L., Shi, L. et al., "Effects of Control Strategies of the Electric Supercharger on Transient Processes of a Turbocharged Diesel Engine," *Energy* (2024): 132427.
33. Serrano, J.R., Climent, H., Piqueras, P., and Darbhamalla, A., "Energy Recovery Potential by Replacing the Exhaust Gases Recirculation Valve with an Additional Turbocharger in a Heavy-Duty Engine," *Energy Conversion and Management* 271 (2022): 116307.
34. Zhang, F., Wang, Z., Tian, J., Li, L. et al., "Effect of EGR and Fuel Injection Strategies on the Heavy-Duty Diesel Engine Emission Performance under Transient Operation," *Energies* 13, no. 3 (2020): 566.
35. Gumus, E. and Otkur, M., "Design of an Optimum Compact EGR Cooler in a Heavy-Duty Diesel Engine towards Meeting Euro 7 Emission Regulations," *Sustainability* 15, no. 16 (2023): 12361.
36. Bitsis, D., Matheaus, A., Hopkins, J., and McCarthy, J. Jr., "Improving Brake Thermal Efficiency Using High-Efficiency Turbo and EGR Pump While Meeting 2027 Emissions," SAE

Downloaded from SAE International by Purdue University Technical Papers, Wednesday, March 12, 2025

Technical Paper 2021-01-1154 (2021), doi:https://doi.org/10.4271/2021-01-1154.

37. Ahmad, Z., "Optimizing Fuel Economy and Emissions for Off-Road Diesel Engine Using Electric EGR Pump and High Efficiency Turbo," Masters thesis, School of Mechanical Engineering, Purdue University, West Lafayette, IN, 2023, https://hammer.purdue.edu/authors/Zar_Nigar_Ahmad/17552235.
38. Ahmad, Z.N., Kakani, R., Willoughby, A., Adekanbi, M. et al., "Impact of Off-Road Engine Electrification through EGR Pumping on CO_2, Soot, and NOx Emissions Reductions during Steady-State Operating Conditions," *International Journal of Engine Research*, 2024, 14680874241280707.
39. Starnes, D.S., Yates, D., and Moore, D.S., *The Practice of Statistics* (W.H. Freeman and Company, New York, USA, 2010)
40. CIMAC, "Turbocharging Efficiencies - Definitions and Guidelines for Measurement and Calculation," The International Council on Combustion Engines, 2007.

© 2024 SAE International. All rights reserved. No part of this publication may be reproduced, stored in a retrieval system, transmitted, in any form or by any means, electronic, mechanical, photocopying, recording, or otherwise, or used for text and data mining, AI training, or similar technologies, without the prior written permission of SAE.

Positions and opinions advanced in this work are those of the author(s) and not necessarily those of SAE International. Responsibility for the content of the work lies solely with the author(s).

Downloaded from SAE International by Purdue University Technical Papers, Wednesday, March 12, 2025